Lightweight crash energy absorber design using composite materials

S. Mantovani, M. Cavazzuti, E. Torricelli
MilleChili Lab
Università degli Studi di Modena e Reggio Emilia
Modena, Italy
millechililab@unimore.it

P. Fabbri
Dipartimento di Ingegneria dei Materiali e dell'Ambiente
Università degli Studi di Modena e Reggio Emilia
Modena, Italy

Abstract—**In an ongoing effort to increase the effectiveness of crash energy absorbers, thus improving the safety performance of cars, the interest in automotive industry in exploring lightweight alternatives to aluminum is deepening. In view of weight reduction, the research on composite materials has grown quickly because of their higher energy absorption-to-weight ratio. In the present work fiberglass composites with different shapes, types of fiber and stacking sequence are considered and analyzed by means of experiments and numerical simulations. At first, tension, compression, and shear properties of the materials are evaluated. Their dynamic properties are also investigated by drop testing according to ASTM D7136 standard. At a later stage, drop-tests are performed on cylindrical composite specimens in order to simulate the crash absorbers dynamic behaviour. Although the cylindrical specimens are not adhering to the standard, the drop tests allow to correlate the experimental data with the numerical simulations. Finally, in the light of the previous dynamic results, the stacking sequence of the composite crash absorbers is numerically optimized by means of design of experiments and optimization techniques for different geometrical shapes. Those considered are simple regular shapes, namely: circular, hexagonal, and octagonal.**

Keywords-composite materials; mechanical properties; crash energy absorbers; optimization techniques; finite element analysis

LIST OF SYMBOLS

E_L	longitudinal Young modulus
G_{LT}	longitudinal transversal shear modulus
ε_{max}	normal yielding strain
γ_{max}	shear yielding strain
σ_c	compression ultimate strength
σ_{max}	normal yielding stress
τ_{max}	shear yielding stress

I. INTRODUCTION

Over the last twenty years, the weight of cars has considerably grown due to the changing needs over time [1]. Passenger comfort, safety standards, structural performance improvements, and the adoption of active and passive security devices are just a few reasons.

However, concerns towards automotive weight reduction are also growing due to the need of complying with the environmental regulations. Besides, car weight reduction also allows a better vehicle handling which is an important factor for high performance sport cars.

The crash absorber is one of the many components for which a careful design approach can take to a fair saving in terms of structural weight. Bumpers and crash absorbers are required to dissipate the highest amount of energy in the event of crash, thus ensuring the passengers safety. Matching the safety requirements and the needs for weight reduction, the interest in composite materials is straightforward for their good mechanical properties compared to their low specific weight. For this reason, composite materials design has driven the attention of many researchers in the automotive industry, also in view of their application to crash absorbers.

Unlike conventional isotropic materials, composite materials properties can vary over a broad range of values. Factors like the manufacturing process, the knowledge of the materials, and their mutual interaction concur in determining the success of a composite component. As a consequence, an accurate characterization of the material properties is also needed.

The improvement of the structural vehicle crashworthiness by adopting Fiber Reinforced Polymers (FRP) composite crash absorbers has been investigated in literature and different types of reinforcements have been addressed. For instance, Mamalis *et al.* [2–3] dealt with shape optimization of fiberglass composite crash absorbers for automotive applications. Failure and collapse modes, and the effect of strain rate were taken into consideration in the absorption mechanism. In recent years, Ochelski *et al.* [4] compared the energy absorption capability

of carbon-epoxy and glass-epoxy composite structures by means of numerical simulations and experiments. The influences of the reinforcement type and of the geometrical shape were investigated. The predictive capability of the numerical models was validated against the experimental results. The energy absorbed by the carbon composite structures is on average 20 % larger compared to the glass composite ones. The comparison between aluminum and composites crash absorbers was carried out by Zarei *et al.* [5] in 2007. Drop tests were conducted on specimens having hexagonal and squared cross-sections. Finite Elements (FE) analyses were used to reveal details about the crash failure mechanisms that occurred during the tests. On the basis of the numerical and the experimental results, a multi-objective optimization was performed to identify the geometry maximizing the energy absorption while minimizing the structural weight. The optimum composite absorber found allowed a 17 % increase in terms of energy absorption together with a 26 % weight reduction compared to the optimum aluminum crash absorber. The development of new manufacturing techniques, such as braiding, has led to consider also the influence of the manufacturing processes over crash absorbers performances. McGregor *et al.* [6] investigated the damage propagation and failure morphology occurring in composite circular and squared tubes. FE models were also implemented in order to capture and predict the behaviour of such structural components. Bisagni *et al.* [7] studied the energy absorption in carbon composite crash absorbers and steering column for Formula One racing cars. A comparison between numerical and experimental results was also made.

Several researches on composite materials are also found in different fields of investigation such as in aerospace. For instance, [8] and [9] deal with crash absorbers for aircraft fuselage structures made of different materials such as carbon composites and Kevlar honeycomb respectively.

The present work presents a methodology for fiberglass crash absorbers design and optimization based on FE simulations in which the material properties definition is tuned after a series of experimental tests. Fiberglass is chosen for its good availability on the market, its price, and manufacturability.

II. Experimental Tests

A woven glass fabric immersed in a polyurethane matrix is taken into consideration in this study. The material is made of a balanced and symmetric lay-up with four layers (unless it is specified differently in the text), obtained through a hand-made lay-up process, and weights 374 g/m2. The material density and reinforcement volume fraction are 2.02 g/cm3 and 62 % respectively. The density is computed without including the void volume fraction. The reinforcement volume fraction is computed from the reinforcement weight and the fiber density, and agrees with the volume fraction expected after a hand lay-up process.

An experimental campaign for assessing the mechanical properties of the material was necessary due to the high variability of such properties that can be found in composite materials. Tab. 1 summarizes the set of experimental tests performed, the standards to which the experiments comply, and the specimen tested. The layers number and orientation varies from test to test as required by the standards.

A. Tensile, Compressive, and Shear Tests

The results of the tensile, compressive, and shear tests are summarized in Tab. 2. The longitudinal strain of the specimens was measured without the use of extensometers by simply tracking the displacement of the movable head. It must be considered that the strain data collected was influenced by the inertial lag of the testing speed, so that the stress-strain curves are slightly affected by error. This was a necessary trade-off choice between accuracy and simplicity.

B. Drop weight test on plates

A drop test was performed over four fiberglass composite plate specimens for measuring the amount of energy dissipated during the impact. The impact energy was set to 15 J in two tests and to 29 J in the other two. The impact mass adopted was weighting 5.73 kg. The displacement and the velocity of the impact mass were recorded at a sampling rate of 819.2 kHz without using a filter dataset. The results of the drop test are also shown in Tab. 2. The glass composite material tested has an excellent deformation recovery.

III. Numerical/Experimental Correlation

The data collected during the experimental tests was used for the definition of the material properties in the FE analyses of a drop test over a fiberglass composite thin-walled cylinder. Since the experimental data was not sufficient to fill the material card in the FE solver, a sensitivity analysis was performed on the remaining parameters, and the most significant were tuned iteratively so that the numerical energy absorption curve was matching the experimental one closely enough.

A. Drop weight test on cylinders

As a consequence, more experimental tests were necessary and were performed on the composite cylinders summarized in Tab. 3. Due to the limits of the drop test machine available, the cylinders testing did not follow any standard, and a stiff steel

TABLE I. Summary of the Experimental Tests Performed

Exp #	Test	Referential Standard	Cross-Section	Movable Head Displacement
1	Tensile	ASTM D3039	Constant Rectangular	2.0 mm/min
2	Compressive	ASTM D3410	Constant Rectangular	1.5 mm/min
3	Compressive	ASTM D3410	Constant Rectangular	1.5 mm/min
4	Shear	ASTM D3518	Constant Rectangular	2.0 mm/min
5	Drop weight	ASTM D7136	Flat Rectangular Plate	N./A.

TABLE II. MATERIAL CHARACTERIZATION AFTER THE EXPERIMENTS

Tensile Test				
Exp #	E_L	σ_{max}	ε_{max}	***Strain Energy Density at Failure***
1	19.1 GPa	446.6 MPa	0.04 mm/mm	16.4 J
Compressive Test				
Exp #	σ_c			***Failure Mode***
2	212.0 ± 28.8 MPa			Crack
3	68.7 ± 8.0 MPa			Buckling
Shear Test				
Exp #	G_{LT}	τ_{max}	γ_{max}	***Strain Energy Density at Failure***
4	7.6 GPa	142.9 MPa	0.37 mm/mm	53.6 J
Drop Test				
Exp #	***Impact Energy***	***Dissipated Energy***	***Maximum Deflection***	***Residual Deflection***
5	14.93 J	14.98 J	7.32 mm	4.40 mm (–39.9 %)
6	29.07 J	25.74 J	16.14 mm	8.05 mm (–50.1 %)

plate was needed in between the cylindrical specimens and the weight since the cylinders diameter was larger than the drop weight diameter.

The glass reinforcement was rolled up around a thick paperboard to avoid undesired deformations in the specimens resin curing and cutting process.

B. *Numerical model setup*

The solver RADIOSS-Block90 was used for the numerical simulations of the drop weight test over the cylinders. The composite material was modeled using shell elements with elastoplastic orthotropic properties (LAW25). The Tsai-Wu failure criterion, which allows the modeling of the material yield and failure phases, was adopted and the artificial hourglass energy was controlled using either the full integration formulation (Q4) or the Quadrilater Elastoplastic Physical Hourglass control (QEPH) with five integration points. The interface between the drop tester, the steel plate, and the specimen was modeled as interface of TYPE7. This choice allows self-contact and the contact on both shell sides to be taken into consideration and prevents the finite elements to penetrate. The friction coefficient was set to 0.2 between the drop weight and the stiff plate, and to 0.4 between the stiff plate and the specimen.

TABLE III. THIN-WALLED CYLINDERS EMPLOYED FOR THE NUMERICAL/EXPERIMENTAL CORRELATION

Exp #	**Internal Diameter**	**Height**	**Thickness**	**Stacking Sequence**	**Impact Energy**
6	39.0 mm	50.0 mm	≈ 1.9 mm	$[45°,–45°]_s$	47.3 J
7	39.0 mm	34.5 mm	≈ 1.9 mm	$[45°,–45°]_s$	48.7 J
8	39.0 mm	34.5 mm	≈ 2.6 mm	$[45°,–45°,45°]_s$	48.6 J
9	39.0 mm	34.5 mm	≈ 2.6 mm	$[45°,–45°,45°]_s$	188.5 J

C. *Numerical/Experimental Comparison*

Fig. 1 shows the results of the drop weight experiments and of the corresponding numerical simulations for the four cases in Tab. 3. Numerical analyses were performed using both Q4 and QEPH formulations for hourglass control, only the latter results are shown for brevity. QEPH gives a better correlation, even though the differences between the two formulations are usually quite small. Experimental data shows that:

- the energy absorption history is influenced by the specimen thickness. In fact, as the thickness is increased the impact energy is dissipated more quickly (see specimens #7 and #8),
- after approximately 4 ms the energy has been completely dissipated for all the cases,
- the flat parts in the experimental energy absorption curves are typical responses due to the generation of the folding deformations,
- the initial folding is detected close to the top end of the specimen (see Fig. 2).

The numerical simulations are able to detect correctly all of the above behaviours but the influence of the folding deformations over the energy absorption history. The numerical model appears less stiff since the numerical and the experimental maximum outer diameter of the deformed shapes in Fig. 2 are 45.28 mm and 44.65 mm respectively, while the undeformed outer diameter of the models is 42.93 mm. This relatively large difference (+36 % on the deformation magnitude) is due to the fact that in the numerical model it was not possible to constrain the rotation of the nodes of the specimen top section because of the shell elements formulation in the FE solver. On the other hand, the specimen length subject to deformation, computed from the top section, is

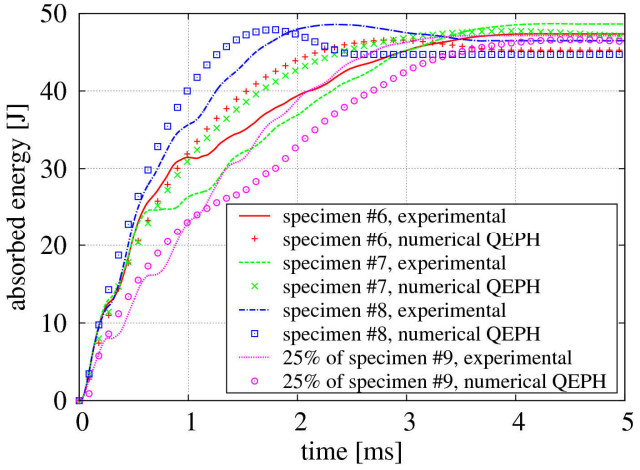

Figure 1. Numerical/experimental correlation: energy absorption history.

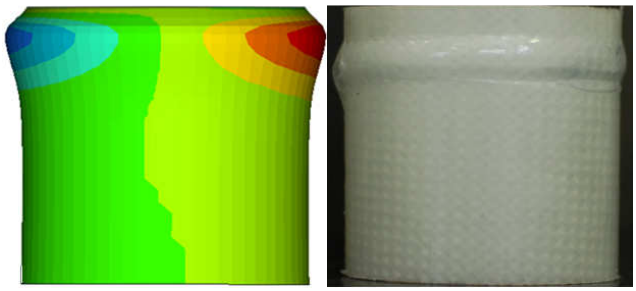

Figure 2. Numerical/experimental correlation: deformed shapes for specimen #6

almost the same among the two cases being 13.75 mm in the experiment and 13.80 mm in the numerical simulation.

IV. Optimization of Fiberglass Crash Energy Absorbers

The numerical model, calibrated as described in the previous paragraphs was finally used in conjunction with optimization techniques in order to find the optimum stacking sequence of both the cylindrical specimens and three types of crash energy absorbers. The objective of the optimization was the maximization of the energy dissipated by the components while the variables were the orientation of their plies. For setting up the process the optimization software modeFRONTIER has been coupled to the solver RADIOSS-Block90 by means of a routine written in C++.

A. Cylindrical specimens optimization

The specimens which were numerically optimized are the same described in Tab. 3 and were crashed at different impact speeds: either 4 m/s or 15 m/s (impact energy of 46 J and 648 J respectively). The fibers orientation was allowed to range from 0 deg to 45 deg with steps of 5 deg. The optimization was performed using a Multi-Objective Genetic Algorithm (MOGA) which was initialized after a Multi-Objective Game Theory (MOGT) algorithm run. Tab. 4 resumes the specimens tested and shows the results in terms of optimum lay-up and energy ratio absorbed by each ply. The plies are reported starting from the inner to the outer one. Tab. 4 shows how the optimum stacking sequence depends both on the crash energy level (see #10 and #11), and on the specimen aspect ratio (see #11 and #12). In particular, the fiber orientation angle is increased in #11 in order to protect the specimen from buckling.

B. Crash energy absorbers optimization

An optimization process was applied to three fiberglass crash energy absorbers having different cross-sections, namely: circular, hexagonal, and octagonal. For simplicity, only four-ply composite components were considered. The optimization process applied is somewhat nontraditional in that it makes no use of optimization algorithms in the strict sense of the word, but is based on the exploration of the design space by means of Design Of Experiments (DOE) techniques coupled with Response Surface Modeling (RSM). At first a 600 simulations Sobol' DOE was performed. DOE data were then interpolated with a Gaussian RSM, and a 10 levels Full Factorial (FF) DOE was applied on the response surface for locating the peaks in the design space. Since the ply orientation was allowed to vary between 0 deg and 45 deg with steps of 5 deg, the possible values each ply can assume are 10, thus, a 10 levels FF corresponds to the exploration of the entire design space through the response surface. The virtual peaks in the response surface were then evaluated by simulation to check their consistency, and the numerical local optimums were found by means of local star points searches.

The crash absorbers weighted 308 g and were placed in between a stationary rigid wall and rigid body elements transmitting a load of 400 kg moving at an initial speed of 40 m/s. The length of the crash absorbers was 0.5 m, and the size of the cross-sections was chosen so that in the three cases the inertia of the sections was the same (diameter of approximately 80 mm) while their overall thickness was 1.87 mm. Tab. 5 resumes the optimum ply lay-up found for the three crash absorbers and the energy ratio absorbed per ply starting from the inner ply. The octagonal geometry has shown to be the most performing; additionally it also causes the deformation to propagate more neatly. Compared to an aluminum crash absorber having the same shape, the fiberglass octagonal crash absorber has a weight 51 % lower and specific energy absorption after 10 ms only 4 % lower. The deformed shapes of the three composite crash absorbers are shown in Fig. 3.

V. Conclusions

A fiberglass composite material was characterized and a numerical-experimental correlation for cylindrical specimens was found. The correlation was applied for setting up the material properties in a numerical model which underwent an optimization process aiming at finding the optimum lay-up for a four-ply fiberglass composite automotive crash absorber. The optimum octagonal crash absorber allows specific energy

TABLE IV. Optimized Specimens, Optimum Lay-Up, and Energy Ratio Absorbed per Ply. The Internal Diameter is 39 mm for every Specimen

Exp #	Height	Ply #	Impact Speed	Optimum Stacking Sequence	Energy Ratio Absorbed per Ply					
					1st	*2nd*	*3rd*	*4th*	*5th*	*6th*
10	50.0 mm	4	4 m/s	[20°,10°,10°,10°]	6.4 %	17.0 %	25.5 %	51.1 %	–	–
11	50.0 mm	4	15 m/s	[15°,45°,20°,10°]	22.7 %	19.4 %	1.7 %	56.2 %	–	–
12	34.5 mm	4	15 m/s	[0°,15°,5°,0°]	25.6 %	36.6 %	11.2 %	26.7 %	–	–
13	34.5 mm	6	15 m/s	[5°,5°,0°,5°,0°,10°]	12.7 %	5.4 %	15.4 %	16.4 %	26.2 %	23.9 %

TABLE V. OPTIMUM CRASH ABSORBERS: LAY-UP AND ENERGY RATIO ABSORBED PER PLY

Cross-Section	Impact Speed	Optimum Stacking Sequence	Absorbed Energy after 10 ms	Specific Energy	Energy Ratio Absorbed per Ply			
					1st	*2nd*	*3rd*	*4th*
Circular	40 m/s	[45°,20°,5°,15°]	6321 J	20.55 J/g	13.6 %	23.7 %	38.6 %	24.0 %
Hexagonal	40 m/s	[40°,25°,40°,35°]	7687 J	24.97 J/g	24.3 %	7.6 %	22.6 %	45.5 %
Octagonal	40 m/s	[5°,5°,0°,15°]	8244 J	26.78 J/g	10.9 %	27.5 %	11.8 %	49.8 %

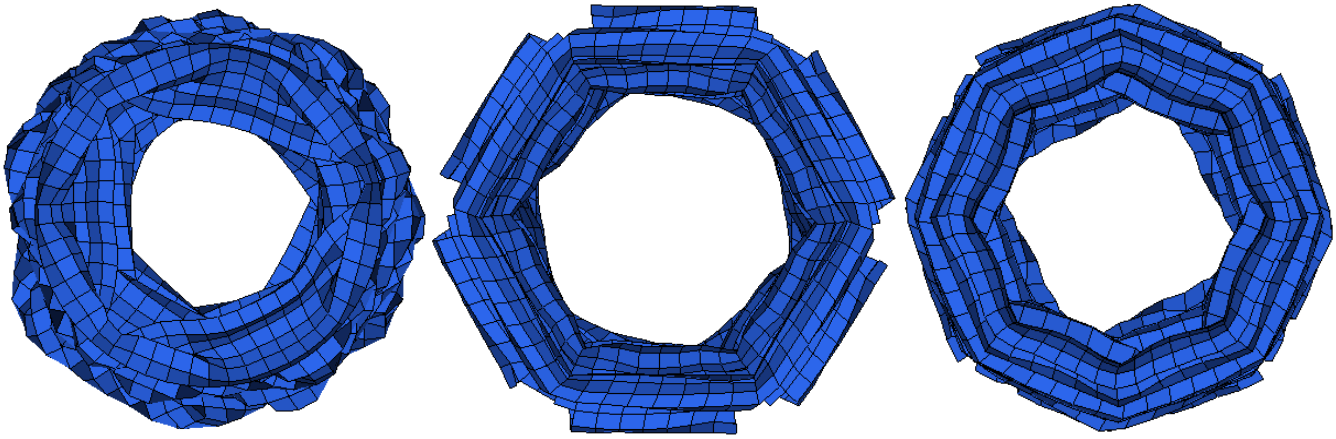

Figure 3. Deformed shapes after crash for the fiberglass composite crash energy absorbers: circular cross-section (left), hexagonal cross-section (centre), and octagonal cross-section (right).

absorption similar to that of an equivalent aluminum crash absorber.

A broader approach to optimization could still be done as a future work involving shape parameters, different ply numbers, and different and more performing composite materials.

REFERENCES

[1] R. Borns, and D. Whitacre, "Optimizing designs of aluminum suspension components using an integrated approach," SAE 05M-2, 2005.

[2] A. G. Mamalis, D. E. Manolakos, G. A. Demosthenous, and M. B. Ioannidis, "The static and dynamic axial collapse of fibreglass composite automotive frame rails," Composite Structures, vol. 34, pp. 77–90, 1996.

[3] A. G. Mamalis, D. E. Manolakos, M. B. Ioannidis, and D. P. Papapostolou, "Crashworthy characteristics of axially statically compressed thin-walled square CFRP composite tubes: experimental," Composite Structures, vol. 63, pp. 347–360, 2004.

[4] S. Ochelski, and P. Gotowicki, "Experimental assessment of energy absorption capability of carbon-epoxy and glass-epoxy composite," Composite Structures, vol. 87, pp. 215–224, 2009.

[5] H. Zarei, M. Kröger, and H. Albertsen, "An experimental and numerical crashworthiness investigation of thermoplastic composite crash," Composite Structures, vol. 85, pp. 245–257, 2008.

[6] C. J. McGregor, R. Vaziri, A. Poursartip, and X. Xiao, "Simulation of progressive damage development in braided composite tubes under axial compression," Composite Part A: applied science and manufacturing, vol. 38, pp. 2247–2259, 2007.

[7] C. Bisagni, G. di Pietro, L. Fraschini, and D. Terletti, "Progressive crushing of fiber-reinforced composite structural components of a formula one racing car," Composite Structures, vol. 68, pp. 491–503, 2005.

[8] S. Heimbs, F. Strobl, P. Middendorf, and J. M. Guimard, "Composite crash absorber for aircraft fuselage applications," in Structures Under Shock and Impact XI, C. A. Brebbia and U. Mander, Eds. WIT Press, 2010, pp 3–14.

[9] E. L. Fasanella, K. E. Jackson, and S. Kellas, "Soft soil impact testing ans simulation of aerospace structures," Proceedings 10th International LS-DYNA Users Conference, 2008.